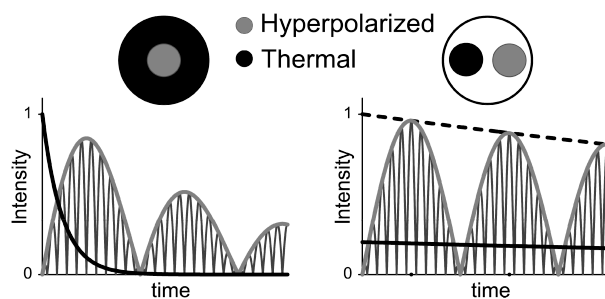


# Proton Magnetic Resonance Imaging with Para-Hydrogen Induced Polarization (Supplementary Information)

Jan F. Dechent, Lisandro Buljubasich, Laura M. Schreiber, Hans W. Spiess and Kerstin Münnemann

## A: Different $T_2^*$ scenarios

Different scenarios must be considered for the presented contrast mechanism concerning transverse relaxation and signal amplitudes, corresponding to different commonly encountered situations. Here we treat the cases of A.1: the thermal background having a smaller  $T_2^*$  time than the hyperpolarized substance, A.2: both substances exhibiting similar  $T_2^*$  times, and A.3: the hyperpolarized signal is smaller than the signal of the background.



**Figure S1:** Time domain evolution of the FIDs for thermal water (black) and antiphase hyperpolarized substance (gray) at different  $T_2^*$  conditions. Left: Fast decaying thermal signal. The contrast will be supported by the  $T_2^*$  effect. Right: Same  $T_2^*$  conditions. Hyperpolarization should exceed thermal polarization to generate a contrast (dashed line: same amount of polarization; solid line: gives rise to contrast).

### A.1: Fast decaying thermal signal

Here we consider the case; where the hyperpolarized molecules are spatially confined and surrounded by a large volume of thermally polarized molecules, see Figure S1 (left). The inner region in gray represents the PHIP molecules whereas the black surrounding region corresponds to the thermal background.

If the small region containing hyperpolarized molecules is placed in the middle of the magnet, where the magnetic field is more homogeneous, a smaller transverse relaxation effect is expected compared to the background molecules, resulting in a noticeable difference in  $T_2^*$ . Moreover, conformal voxel shimming can be applied to obtain an even larger  $T_2^*$  in the hyperpolarized area.<sup>1</sup>

The time evolution of the magnitude signals of both, the hyperpolarized and the thermal regions, are also included in Figure S1 (left). Notice that due to the fast  $T_2^*$  relaxation in the thermally polarized area,

the thermal signal (solid black line) has almost completely decayed when the hyperpolarized signal (solid grey line) reaches the first maximum due to the J-coupling induced refocusing. These two effects work together in rendering the contrast between the two regions. In Figure S1 (left) we assumed that the overall maximum of the hyperpolarized signal is roughly equal to the total amount of initial thermal polarization. This example shows, that for the beneficial case where the hyperpolarized substances possesses a longer  $T_2^*$  than the thermal background, the total intensity of the PHIP signal can be even smaller than the one of the thermal background, allowing for the detection of a very small concentration of the PHIP substance. We hurry to point out that for the sake of clarity, the  $T_2^*$  difference was exaggerated in the figure. In general it seems to be better to delay the acquisition until the second maximum to obtain the highest contrast. The best condition will, however, depend on the relaxation effects combined with the evolution under the J-coupling and chemical shift Hamiltonian of the hyperpolarized molecules used.

### A.2: Same $T_2^*$ conditions

Here we consider the case in which both hyperpolarized and thermally polarized molecules experience similar  $B_0$  inhomogeneities, thus exhibiting the same  $T_2^*$ . This could be the case for either two spatially separated regions placed in parts of the magnetic field presenting similar  $B_0$  inhomogeneities, or only one region where the PHIP molecules are distributed in the thermal environment. The setup corresponding to the spatially separated regions is shown in Figure S1 (right), along with the time evolution of the respective magnitude signals.

The dashed line shows the decay of the thermal signal, where the total amount of hyperpolarization is considered equal to the initial thermal polarization, like in the sketch for case A.1. Notice that no contrast is obtained in such a situation. However, if the hyperpolarized signal is assumed to be larger than the total thermal signal (see the solid black line in Figure S1 (right)), the maximum contrast is obtained at the first maximum of the PHIP signal. This condition can be easily met in PHIP hyperpolarization studies due to the large enhancements obtained as is shown by the experimental results in the manuscript. It establishes, nevertheless, a condition for the minimum amount of PHIP molecules with respect to the thermal molecules necessary to differentiate the signals. This minimum is obviously higher compared to case A.1, and could be critical, deciding on the viability of the application to MRI.

### A.3: Same $T_2^*$ conditions and small hyperpolarization

If both liquids have the same  $T_2^*$  and the amount of hyperpolarization is equal or even smaller than the initial thermal polarization, we encounter the most disadvantageous situation, see Figure S2 and recording a single image is not sufficient to generate sufficient contrast. As is well-known in MRI, contrast can be improved by taking differences of images recorded under different conditions.<sup>2,3</sup> In our case it is sufficient to simply acquire two images with different delays as marked in Figure S2 as M1 and M2, respectively. For the first image, the thermal polarization is almost maximum whereas the PHIP contribution is almost zero. The second image will contain the maximum contribution from the hyperpolarized material along with still almost full thermal polarization. By subtracting the first image from the second one, an acceptable contrast can be obtained. Note that the procedure relies on the fact that while the PHIP signal increases due to the J-coupling evolution, the thermal signal decreases (as both  $T_2^*$  are equal, it is also possible to remove that factor from the analysis, resulting in an increasing

PHIP signal and a constant thermal signal). Although the fact that the thermal molecules are on-resonant helps for the analysis, this condition is not restrictive at all.

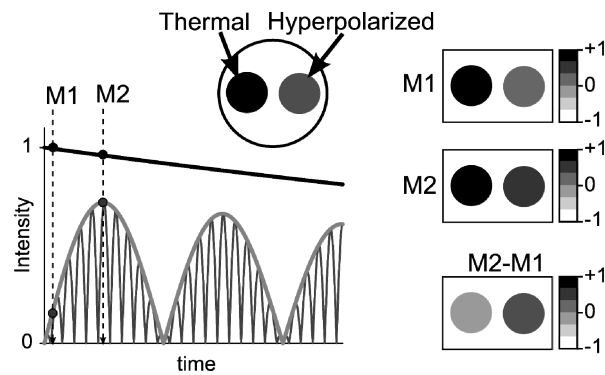


**Figure S2:** Time domain evolution of FID for thermal water (black) and antiphase hyperpolarized substance (gray) at same  $T_2^*$  conditions. The thermal polarization exceeds the hyperpolarized polarization. Subtraction images (right) at two favorable echo times allows for separation of the two areas by sign.

If the thermal signal is not perfectly on-resonant, the oscillation will introduce only minor changes. Nevertheless, independent of the resonance condition, the thermal difference image will present negative intensity, while the value from the PHIP molecules will be always positive. The acquisition of two images instead of one is of course a drawback for *in vivo* MRI because co-registration problems could occur. However, this is also true for MRI of  $^{13}\text{C}$  hyperpolarized substances where co-registration with a proton image is needed to provide anatomical information. Moreover in our case, this problem can be easily solved by applying a multi-echo sequence and subtracting two images with different echo times.

## B: Experimental Details

### Acquisition:

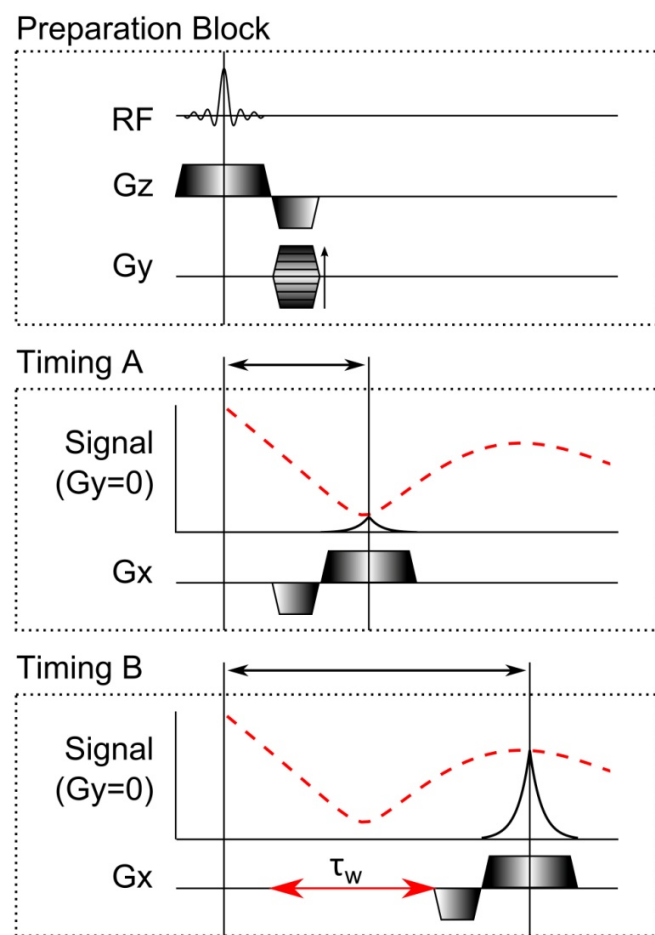
Imaging experiments were performed in a 1.5 Tesla imaging system (Magnetom Sonata, Siemens Medical, Erlangen, Germany). For signal acquisition a finger coil (small loop coil, Siemens Medical, Erlangen, Germany) with 3 cm inner diameter was used. All filter algorithms were deactivated. The resonance frequency, transmitter and shim of the system were calibrated using a water filled NMR tube. For evaluating the amount of initial hyperpolarization an FID (flip angle: 10°, bandwidth: 10000Hz, vector size: 2048) was acquired prior to each image. The imaging experiments followed subsequently using a gradient echo sequence with variable waiting time (flip angle: 10°, repetition time case (i): 45 ms, repetition time case (ii): 65 ms, bandwidth per pixel: 600 Hz, FOV: 50 mm<sup>2</sup>, resolution: 0.7 mm/Pixel and total acquisition time: 3.96 s). K-space raw data of each experiment were stored.

### Sequence:

The MRI experiments were performed with the gradient echo sequence FLASH [A. Haase, J. Frahm, D. Matthaei, W. Haenische, K.-D. Merboldt, FLASH imaging, rapid NMR imaging using low flip angle pulses, *J. Magn. Reson.* 67 (1986) 258–266] depicted in the figure on the right. The preparation block contains the excitation by a soft radio frequency pulse (RF) combined with a slice selective magnetic field gradient (Gz) as well as phase encoding in the y direction (Gy). Two possible timings (A and B) between excitation and readout gradient (Gx) are presented. The signals depicted for both cases represent the absolute value of magnetization in the transverse plane. The red dashed line depicts the FID of our sample (compare Figs. 2 and 4). At the center of the positive-lobed readout gradient the dephasing introduced by gradients along the read direction is zero, thus leading to a signal with exactly the same height as the FID ( $k_x=k_y=0$ ). Timing A is optimal for the acquisition of thermal signals, whereas the contribution from the antiphase hyperpolarization is suppressed. Timing B includes an additional waiting time ( $\tau_w$ ); resulting in refocusing of the antiphase magnetization at the time point of acquisition yielding high MRI signals.

### Postprocessing:

Imaging data were first processed with a Gaussian filter of half width in each direction; afterwards zero filling of factor 2 was applied. After Fourier transformation



the images were depicted only showing the relevant area of the phantom tube, but not excluding possible artefacts. MR images are presented without correction of initial hyperpolarization. SNR-maps are calculated by dividing each pixel by  $(2/\pi)^{1/2}$  and the mean value of the noise. The noise is calculated from an area far outside the phantom. Two regions of interest (ROI) were chosen, one laying inside the hyperpolarized area the other within the area of thermal polarization.

The SNR value of the hyperpolarized area can be corrected by the initial hyperpolarization by dividing with the corresponding factor ( $cf_i$ ). Therefore, the initial polarization was calculated by the integral of the absolute fid and subtracted by a thermal reference fid:

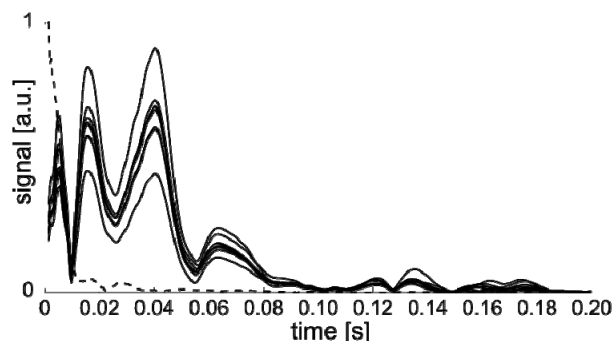
$$|f_i| = \int |signal_{hyperpolarized} - signal_{thermal}|$$

The correction factors  $cf_i$  are  $f_i$  divided by the mean value of all  $f_i$ .

$$cf_i = f_i / \bar{f}_i$$

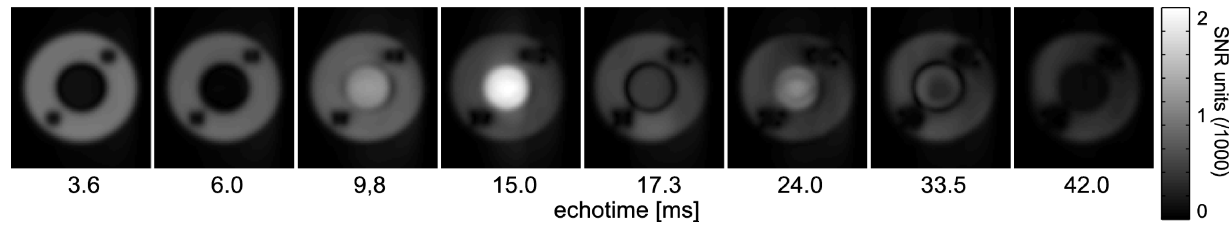
This presentation allows an intuitive understanding of the huge signal intensities being at hand.

### C: Several FIDs of hyperpolarized Hexene



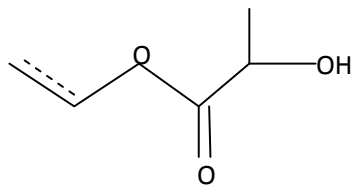
Time domain signal of hyperpolarized hexene (solid line). Each solid line corresponds to the available hyperpolarization of the images (Figure 4) and high reproducibility of PHIP hyperpolarization throughout the image series can be seen. Thermal signal (dashed line) is given as reference.

#### D: PHIP-Imaging with 2-Hydroxyethylpropionate



MR-images of hyperpolarized PHIP substance (2-Hydroxyethylpropionate) and thermal water within the phantom for case (i) acquired at different echo times by individual experiments. Same parameters and explanation as for Figure 4 of the main text are holding. We obtain also with this substance excellent MRI contrast showing the generality of our approach.

Chemical Structure: 2-Hydroxyethylpropionate (2-Hydroxyethylacrylate with dashed line)



## E: Additional References

1. R. Gruetter, *Magn. Reson. Med.*, 1993, **29**, 804-811.
2. H. Ersoy and F. J. Rybicki, *Am. J. Roentgenol.*, 2008, **190**, 1675-1684.
3. A. Newatia, G. Khatri, B. Friedman and J. Hines, *Am. J. Roentgenol.*, 2007, **188**, 1018.
4. D. Canet, S. Bouquet-Bonnet, C. Aroulanda and F. Reineri, *J. Am. Chem. Soc.*, 2007, **129**, 1445-1449.